Diffusiophoresis of a Soft Sphere Normal to Two Parallel Disks

ARTICLE *in* LANGMUIR · OCTOBER 2010

Impact Factor: 4.46 · DOI: 10.1021/la102631q · Source: PubMed

5 AUTHORS, INCLUDING:

Wei-Lun Hsu
The University of Tokyo
17 PUBLICATIONS **128** CITATIONS
SEE PROFILE

Li-Hsien Yeh
National Yunlin University of Science and Te…
62 PUBLICATIONS **702** CITATIONS
SEE PROFILE

Langmuir Article

pubs.acs.org/Langmuir

Diffusiophoresis of a Soft Sphere Normal to Two Parallel Disks

Jyh-Ping Hsu,* Kuan-Liang Liu, Wei-Lun Hsu, and Li-Hsien Yeh

Department of Chemical Engineering, National Taiwan University, Taipei, Taiwan 10617

Shiojenn Tseng

Department of Mathematics, Tamkang University, Tamsui, Taipei, Taiwan 25137

Received June 30, 2010. Revised Manuscript Received August 20, 2010

The diffusiophoresis of a soft spherical particle normal to two parallel disks subject to an applied ionic concentration gradient is modeled theoretically. The soft particle, which comprises a rigid core and a porous membrane layer, is capable of simulating a wide class of particles such as biocolloids and particles covered by an artificial membrane layer; a rigid particle can also be recovered as the limiting case where the membrane layer is infinitely thin. The problem considered simulates, for example, the chemotaxis of cells or microorganisms. We show that the presence of the membrane layer is capable of yielding complicated diffusiophoretic behavior when the sign of the charge carried by that layer is different from that on the surface of the rigid core of the particle. Both the sign and the magnitude of the diffusiophoretic velocity of a particle can be adjusted through varying the friction coefficient of its membrane layer. These results are of practical significance, for example, in the case where diffusiophoresis is adopted as a separation operation or as a tool to carry and/or control the rate of drug release.

Introduction

When a spherical charged colloidal particle is immersed in an electrolyte solution, the concentration of counterions near its surface is higher than that of co-ions, forming a spherical electrical double layer with its thickness roughly inversely proportional to the square root of the bulk electrolyte concentration. The double layer becomes asymmetric; however, if an electrolyte concentration gradient is applied, where it is thinner (thicker) on the high- (low-) concentration side of the particle. The asymmetric double layer induces a local electric field driving the particle toward the high-concentration side, known as diffusiophoresis. Diffusiophoresis also includes the case where an uncharged particle is driven by an applied concentration gradient of nonelectrolyte.[1] In practice, diffusiophoresis has been adopted as a separation tool,[2] as a process to deposit particles on a surface,[3] and in surface coating.[4] Without the necessity of a second metal in electrical contact,[5] or the Joules heat effect,[6] diffusiophoresis is also taken as a novel driving mechanism for catalytic micromotors[7,8] or pattern formation[9] recently. Diffusiophoresis also plays an important role in biological science. A typical example includes chemotaxis, the movement of cells and microorganisms driven by a concentration gradient of chemicals such as nutrients and toxic species.[10−12]

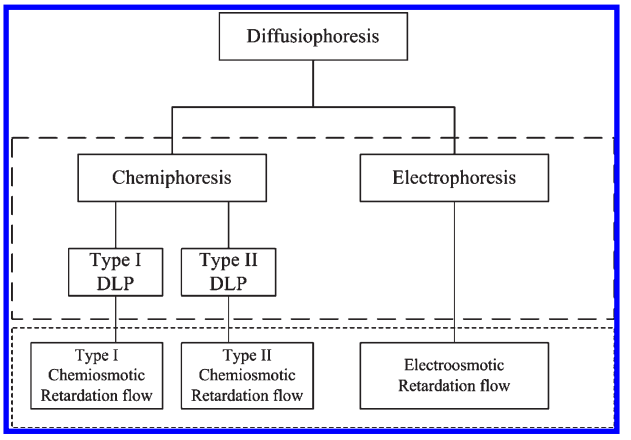

Figure 1. Mechanisms involved in the diffusiophoresis of a particle in an electrolyte solution. Longer dashed frame: electrical elements. Shorter dashed frame: hydrodynamic elements.

Referring to Figure 1, if diffusiophoresis is conducted in an electrolyte medium, then several mechanisms are involved. Chemiphoresis, one of the two main driving mechanisms of diffusiophoresis, comes from the asymmetric concentration distribution of ionic species in the presence of an applied electrolyte concentration gradient, known as double-layer polarization (DLP).[13] Hsu et al.[14] suggested the presence of two types of DLP. Type I DLP[13] occurs inside the double layer, where the concentration of counterions on the high-concentration side is higher than that on the low-concentration side, yielding a local electric field driving the particle toward the high-concentration side, regardless of the sign of its charge. Immediately outside the double layer, the concentration of co-ions on the high-concentration side is higher than that on the low-concentration side, yielding a local electric

*To whom correspondence should be addressed. Telephone: 886-2-23637448. Fax: 886-2-23623040. E-mail: jphsu@ntu.edu.tw.

(1) Keh, H. J.; Wan, Y. W. *Chem. Eng. Sci.* **2008**, *63*, 1612.
(2) Meisen, A.; Bobkowic, A. J.; Cooke, N. E.; Farkas, E. J. *Can. J. Chem. Eng.* **1971**, *49*, 449.
(3) Munoz-Cobo, J. L.; Pena, J.; Herranz, L. E.; Perez-Navarro, A. *Nucl. Eng. Des.* **2005**, *235*, 1225.
(4) Dvornichenko, G. L.; Nizhnik, Y. V.; Slavikovskii, T. V. *Colloid J. Russ. Acad. Sci.* **1993**, *55*, 36.
(5) Kline, T. R.; Paxton, W.; Wang, Y.; Velegol, D.; Mallouk, T. E.; Sen, A. *J. Am. Chem. Soc.* **2005**, *127*, 17150.
(6) Knox, J. H.; Mccormick, R. M. *Chromatographia* **1994**, *38*, 207.
(7) Sen, A.; Ibele, M.; Hong, Y.; Velegol, D. *Faraday Discuss.* **2009**, *143*, 15.
(8) Chaturvedi, N.; Hong, Y.; Sen, A.; Velegol, D. *Langmuir* **2010**, *26*, 6308.
(9) Palacci, J.; Abecassis, B.; Cottin-Bizonne, C.; Ybert, C.; Bocquet, L. *Phys. Rev. Lett.* **2010**, *104*, 138302.
(10) Parent, C. A.; Devreotes, P. N. *Science* **1999**, *284*, 765.
(11) Dekker, L. V.; Segal, A. W. *Science* **2000**, *287*, 982.
(12) Prieve, D. C. *Nat. Mater.* **2008**, *7*, 769.
(13) Zhang, X. G.; Hsu, W. L.; Hsu, J. P; Tseng, S. J. *J. Phys. Chem. B* **2009**, *113*, 8646.
(14) Hsu, J. P.; Liu, K. L.; Hsu, W. L.; Yeh, L. H.; Tseng, S. J. *J. Phys. Chem. B* **2010**, *114*, 2766.

field, the direction of which is opposite to that induced by type I DLP, known as type II DLP.[14] If the diffusivity of cations is different from that of anions, then the application of a concentration gradient yields a background electric field and, depending upon the sign of the charge on the particle surface, it can be driven toward either the high- or the low-concentration side,[15] known as the electrophoresis effect. The effects of type I DLP, type II DLP, and electrophoresis all contribute to the electric force acting on the particle. The relative significance of these effects depends upon the charged conditions of a particle, the thickness of double layer, the type of electrolytes in the solution, and whether a boundary is present.[14−16] Inside the double layer surrounding a particle, because counterions are more abundant than co-ions, the direction of the fluid flow is opposite to that of the particle motion. That is, an osmotic retardation flow is present, yielding a hydrodynamic drag force acting on the particle. As summarized in Figure 1, three types of retardation flow are present; each comes from one of the effects mentioned above.

Soft or fuzzy particle model, where a particle comprises a rigid core and a porous layer, can be used to simulate a wide class of particles of nonrigid nature.[17−21] For instance, biocolloids are usually mimicked by a rigid core covered by an ion-penetrable, charged membrane layer,[13,22−24] and inorganic colloidal particles often bear an artificial polymer layer to prevent them from aggregation.[25−28] The presence of a porous layer of a soft particle is capable of influencing significantly its electrokinetic behavior, especially when its rigid core and porous layer bear charges of different sign.[29−33] Note that, for rigid particles, the osmotic hydrodynamic force acting on a particle in diffusiophoresis is usually less important than the electric force.[14−16] However, for soft particles, due to the friction of the porous layer, that force can play a role.

In this study, the diffusiophoresis of a charged particle covered by an ion-penetrable membrane layer in an electrolyte solution normal to two large, parallel disks is modeled. Through the geometry considered, we can examine the presence of a boundary on the diffusiophoretic behavior of a biocolloid. The adhesion of leukocyte to a wounded tissue surface driven by chemotaxis, for example, can be simulated by the present problem. The equations governing the diffusiophoretic behavior of the particle are solved numerically subject to prespecified boundary conditions by *FlexPDE*,[34] a finite element method based commercial software. Numerical simulations are conducted to investigate the influence of the thickness of double layer, the particle-disk distance, the physical properties of the membrane layer, and the diffusivity of ionic species on that behavior.

In the next two sections, we illustrate the mathematical model and the numerical method adopted.

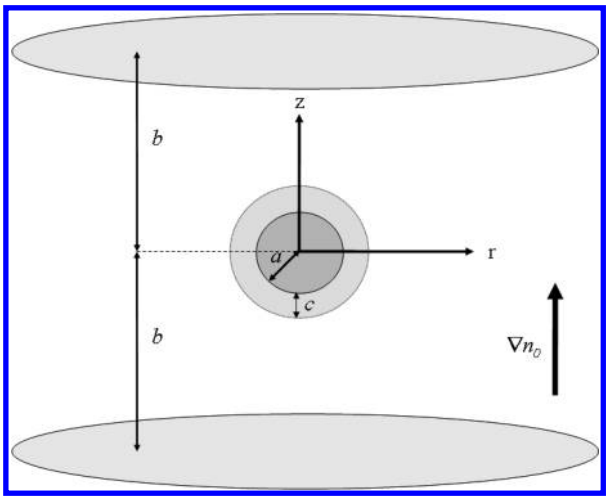

Figure 2. Diffusiophoresis of a soft spherical particle of radius $(a + c)$ comprising a rigid core of radius a and an ion-penetrable membrane layer of thickness c in an electrolyte solution as a response to an applied uniform concentration field ∇n_0 normal to two large parallel disks with half separation distance b; r, θ, z are the cylindrical coordinates adopted with its origin at the center between two disks; ∇n_0 is in the z-direction and the center of the particle at $(z, r) = (0, 0)$.

Modeling

As illustrated in Figure 2, we consider the diffusiophoresis of a soft spherical particle of radius $(a + c)$ comprising a rigid core of radius a and an ion-penetrable membrane layer of thickness c driven by an applied uniform concentration field ∇n_0 normal to two large, parallel disks with half separation distance b. Note that a rigid particle can be recovered from the present soft particle by letting $c \to 0$. The liquid phase between the disks, assumed to be an ideal solution, contains z_1:z_2 electrolytes with z_1 and z_2 being the valences of cations and anions, respectively. Let n_{10} and n_{20} be the bulk concentrations of cations and anions, respectively, and D_1 and D_2 be the corresponding diffusivities. r, θ, and z are the cylindrical coordinates adopted with its origin at the center between two disks. ∇n_0 is in the z-direction, and the center of the particle is at $(z = 0, r = 0)$. Note that the θ-symmetric nature of the present problem suggests that only the (r, z) domain needs be considered. For convenience, we define $\alpha = -z_2/z_1$ and $\beta = (D_1 - D_2)/(D_1 + \alpha D_2)$. The latter is a measure for the difference between the diffusivity of cations and that of anions and, therefore, the degree of electrophoresis effect. For simplicity, we assume that the rigid core of the particle is maintained at a constant potential ζ_a, and the nonreactive membrane layer of the particle contains fixed charge density ρ_{fix}. Let τ be the friction coefficient for the fluid flow inside the membrane layer. We assume that the permittivity ε inside the membrane layer is the same as that outside it and is remained constant, so is the liquid viscosity η. The former is reasonable for polymeric materials having a sufficiently high water content.[20] In addition, we assume that the liquid phase is an incompressible Newtonian fluid. Furthermore, experimental result[9] suggests that the system under consideration can reasonably be assumed to stay at a pseudo steady state.

Suppose that the distribution of ionic species is only slightly distorted over a length scale a after the application of ∇n_0. Then,

(15) Hsu, J. P.; Hsu, W. L.; Chen, Z. S. *Langmuir* **2009**, *25*, 1772.
(16) Hsu, J. P.; Hsu, W. L.; Liu, K. L. *Langmuir* **2010**, *26*, 8648.
(17) Donath, E.; Pastuschenko, V. *Bioelectrochem. Bioenerg.* **1979**, *6*, 543.
(18) Sharp, K. A.; Brooks, D. E. *Biophys. J.* **1985**, *47*, 563.
(19) Ohshima, H.; Kondo, T. *Biophys. Chem.* **1991**, *39*, 191.
(20) Duval, J. F. L.; Ohshima, H. *Langmuir* **2006**, *22*, 3533.
(21) Ohshima, H. *Colloid Polym. Sci.* **2007**, *285*, 1411.
(22) Levine, S.; Levine, M.; Sharp, K. A.; Brooks, D. E. *Biophysis. J.* **1983**, *42*, 127.
(23) Hyono, A.; Gaboriaud, F.; Mazda, T; Takata, Y.; Ohshima, H.; Duval, J. F. L. *Langmuir* **2009**, *25*, 10873.
(24) Ohshima, H.; Makino, K.; Kondo, T. *J. Colloid Interface Sci.* **1987**, *116*, 196.
(25) García-Salinas, M. J.; Romero-Cano, M. S.; Nieves, F. J. *J. Colloid Interface Sci.* **2001**, *241*, 280.
(26) Škvarla, J. *Langmuir* **2007**, *23*, 5305.
(27) Paillard, A.; Passirani, C.; Saulnier, P.; Kroubi, M.; Garcion, E.; Benoit, J. P.; Betbeder, D. *Pharm. Res.* **2009**, *27*, 1.
(28) Gomes, J. P. S.; Rank, A.; Kronenberger, A.; Fritz, J.; Winterhalter, M.; Ramaye, Y. *Langmuir* **2010**, *25*, 6793.
(29) Hsu, J. P.; Chen, Z. S.; Tseng, S. J. *J. Phys. Chem. B* **2009**, *113*, 7701.
(30) Ohshima, H. *J. Colloid Interface Sci.* **2003**, *258*, 252.
(31) Lee, E.; Chou, K. T.; Hsu, J. P. *J. Colloid Interface Sci.* **2004**, *280*, 518.
(32) Cheng, W. L.; He, Y. Y.; Lee, E. *J. Colloid Interface Sci.* **2009**, *335*, 130.
(33) Hsu, J. P.; Kuo, C. C. *Chem. Eng. Sci.* **2009**, *64*, 5247.
(34) *FlexPDE*, version 4.24; PDE Solutions: Spokane Valley, WA, 2004.

the electric potential, ψ, the velocity of the liquid phase relative to the rigid core of the particle, $\mathbf{v}$, the pressure, p, and the number concentration of ionic species j, n_j, can be expressed as $\psi = \psi_e + \delta\psi$, $\mathbf{v} = \mathbf{v}_e + \delta\mathbf{v}$, $p = p_e + \delta p$, $n_j = n_{je} + \delta n_j$.[13,35,36] The subscript e denotes the equilibrium component of a variable and the prefix δ denotes the corresponding perturbed component resulting from the application of ∇n_0. Here, we assume that the fluctuation dissipation theorem[37] is applicable. Since both the particle and the liquid phase are stagnant when ∇n_0 is not applied, $\boldsymbol{v}_e = \mathbf{0}$, and therefore, $\mathbf{v} = \delta\mathbf{v}$. If we let n_{j0} be the bulk concentration of ionic species j, where the subscript 0 denotes the bulk property, then its equilibrium concentration can be described by the Boltzmann distribution, $n_{je} = n_{j0e}\exp[-(z_j e\psi_e)/k_B T]$, $j = 1,2$,[38] where n_{j0e} is the equilibrium bulk concentration of ionic species j. The assumption that n_j is disturbed only slightly by ∇n_0 yields the following set of equations:[14,16,39,40]

$$\nabla^{*2}\psi_e^* = -\frac{(\kappa a)^2}{(1+\alpha)}[\exp(-\psi_e^*) - \exp(\alpha\psi_e^*)] - iQ \quad (1)$$

$$\nabla^{*2}\delta\psi^* = -\frac{(\kappa a)^2}{1+\alpha}[\exp(-\psi_e^*)(\delta\mu_1^* - \delta\psi^*) - \alpha\exp(\alpha\psi_e^*)(\delta\mu_2^* + \delta\psi^*)] \quad (2)$$

$$\nabla^{*2}\delta\mu_1^* = \nabla^*\psi_e^*\cdot\nabla^*\delta\mu_1^* - \gamma Pe_1\mathbf{v}^*\cdot\nabla^*\psi_e^* \quad (3)$$

$$\nabla^{*2}\delta\mu_2^* = -\alpha[\nabla^*\psi_e^*\cdot\nabla^*\delta\mu_2^* - \gamma Pe_2\mathbf{v}^*\cdot\nabla^*\psi_e^*] \quad (4)$$

$$n_1^* = \exp(-\psi_e^*)[1 + \delta\mu_1^* - \delta\psi^*] \quad (5)$$

$$n_2^* = \exp(\alpha\psi_e^*)[1 + \delta\mu_2^* + \alpha\delta\psi^*] \quad (6)$$

In these expressions, $\nabla^* = a\nabla$ and $\nabla^{*2} = a^2\nabla^2$ with ∇ and ∇^2 being the gradient operator and the Laplace operator, respectively. $\psi_e^* = \psi_e/\zeta_a$ and $\delta\psi^* = \delta\psi/\zeta_a$. i is a region index: $i = 1$ denotes the region inside the membrane layer; $i = 0$ denotes the region outside the particle. $\kappa = \{\Sigma_{j=1}^2[n_{j0e}(ez_j)^2/ek_B T]\}^{1/2}$, $Q = \rho_{fix}a^2/\varepsilon\zeta$, $\gamma = \nabla^* n_0^*$, and $Pe_j = \varepsilon\zeta^2/\eta D_j$. $\mathbf{v}^* = \mathbf{v}/U_{ref}$ with $U_{ref} = \varepsilon\gamma\zeta^2/a\eta$ being a reference velocity where $\zeta = k_B T/z_1 e$ is the thermal potential; $n_0^* = n_0/n_{j0e}$ and $n_j^* = n_j/n_{j0e}$. e, k_B, and T are the elementary charge, Boltzmann constant, and the absolute temperature, respectively. $\delta\mu_j^* = \delta\mu_j/k_B T$, with $\delta\mu_j$ being the perturbed electrochemical potential of ionic species j, which can be expressed as[14,41,42]

$$\delta\mu_j = k_B T\frac{\delta n_j}{n_{je}} + z_j e\,\delta\psi \quad (7)$$

The flow field of the present problem can be described by[43]

$$\nabla^*\cdot\mathbf{v}^* = 0 \quad (8)$$

$$-\nabla^*\delta p^* + \gamma\nabla^{*2}\mathbf{v}^* + (\nabla^{*2}\psi_e^* + iQ)\nabla^*\delta\psi^* + \nabla^{*2}\delta\psi^*\nabla^*\psi_e^* - i\gamma(\lambda a)^2\mathbf{v}^* = 0 \quad (9)$$

Here, $\delta p^* = \delta p/p_{ref}$ with $p_{ref} = \varepsilon\zeta^2/a^2$ being a reference pressure; $\lambda = (\tau/\eta)^{1/2}$ is the reciprocal shielding length.

The following boundary conditions are assumed for ψ_e^* and $\delta\psi^*$:

$$\psi_e^* = \zeta_a^* \quad \text{on the surface of the rigid core} \quad (10)$$

$$\mathbf{n}\cdot\nabla\delta\psi^* = 0 \quad \text{on the surface of the rigid core} \quad (11)$$

$$\psi_e^* = 0, \quad Z = \pm b/a \quad (12)$$

$$\mathbf{n}\cdot\nabla\delta\psi^* = \mp\beta r, \quad Z = \pm b/a \quad (13)$$

$$\psi_e^* = 0 \quad \text{as } R \to \infty \quad (14)$$

$$\mathbf{n}\cdot\nabla\delta\psi^* = 0 \quad \text{as } R \to \infty \quad (15)$$

In these expressions, $\mathbf{n}$ is the normal vector directed into the liquid phase; $\zeta_a^* = \zeta_a/\zeta$, $Z = z/a$, and $R = r/a$. Equation 11 implies that the rigid core of the particle is nonconductive, and eq 13 describes the background electric field coming from the difference in the ionic diffusivities.

The following boundary conditions are assumed for $\delta\mu_1^*$ and $\delta\mu_2^*$:

$$\mathbf{n}\cdot\nabla\delta\mu_1^* = 0 \quad \text{on the surface of the rigid core} \quad (16)$$

$$\mathbf{n}\cdot\nabla\delta\mu_2^* = 0 \quad \text{on the surface of the rigid core} \quad (17)$$

$$\delta\mu_1^* = Z\gamma + \delta\psi^*, \; Z = \pm b/a \text{ or as } R \to \infty \quad (18)$$

$$\delta\mu_2^* = Z\gamma - \alpha\delta\psi^*, \; Z = \pm b/a \text{ or as } R \to \infty \quad (19)$$

Equations 16 and 17 imply that the rigid core of the particle is ion-impenetrable, and eqs 18 and 19 come from the assumption that the concentration of ionic species reaches the corresponding bulk level on the boundaries, that is, $n_{j0} = n_{j0e} + z\nabla n_0$.[15]

The nonslip conditions on the surfaces of the rigid core of the particle and the disks, and the fact that the liquid far away from the particle is uninfluenced by its presence,yield the following boundary conditions for $\mathbf{u}^*$:

$$\mathbf{v}^* = 0 \quad \text{on the surface of the rigid core} \quad (20)$$

$$\mathbf{v}^* = -U^*\mathbf{e}_z, \; Z = \pm b/a \text{ or as } R \to \infty \quad (21)$$

Here, $U^* = U/U_{ref}$ with U being the particle velocity; $\mathbf{e}_z$ is the unit vector in the z-direction. In addition, we assume that ψ_e^*, $\mathbf{n}\cdot\nabla\psi_e^*$, $\delta\psi^*$, $\mathbf{n}\cdot\nabla\delta\psi^*$, $\mathbf{n}\cdot\mathbf{v}^*$, $\mathbf{n}\times\mathbf{v}^*$, $\mathbf{n}\cdot(\mathbf{n}\cdot\boldsymbol{\sigma}_H^*)$, $\mathbf{n}\cdot(\mathbf{n}\cdot\boldsymbol{\sigma}_H^*)$, and $\mathbf{n}\times(\mathbf{n}\cdot\boldsymbol{\sigma}_H^*)$ are all continuous on the membrane−liquid interface, where $\boldsymbol{\sigma}_H^* = \boldsymbol{\sigma}_H/[\varepsilon\zeta^2/a^2]$ is the scaled shear stress tensor with $\boldsymbol{\sigma}_H$ being the corresponding shear stress tensor.

(35) Lou, J.; Lee, E. *J. Phys. Chem. C* **2008**, *112*, 2584.
(36) Hsu, J. P.; Lou, J.; He, Y. Y.; Lee, E. *J. Phys. Chem. B* **2007**, *111*, 2533.
(37) Callen, H. B.; Welton, T. A. *Phys. Rev.* **1951**, *83*, 34.
(38) Hunter, R. J. *Foundations of Colloid Science*; Oxford University: Oxford, 1989; Vol. *1*.
(39) Lee, E.; Chu, J. W.; Hsu, J. P. *J. Colloid Interface Sci.* **1998**, *205*, 65.
(40) Hsu, J. P.; Yeh, L. H.; Ku, M. H. *J. Colloid Interface Sci.* **2007**, *305*, 324.
(41) Prieve, D. C.; Roman, R. *J. Chem. Soc., Faraday Trans. II* **1987**, *83*, 1287.
(42) Keh, H. J.; Li, Y. L. *Langmuir* **2007**, *23*, 1061.
(43) Masliyah, J. H.; Bhattacharjee, S. *Electrokinetic Transport Phenomena*, 4th ed.; Wiley: New York, 2006.

Let $\mathbf{F}$ and F be the total force acting on the particle in the z-direction and its magnitude, respectively. Two types of force need be considered in our case, namely, the electrical force $\mathbf{F_e}$ with magnitude F_e and the hydrodynamic force $\mathbf{F_d}$ with magnitude F_d. The steady state assumption implies that $(F_e + F_d)$ must vanish, which can be used to evaluate the diffusiophoretic velocity of the particle U. This, however, involves a trial-and-error procedure. Similar to the treatment of O'Brien and White,[44] this difficulty can be avoided by decomposing the original problem into two subproblems: in the first subproblem, the particle moves with a constant velocity in the absence of ∇n_0, and in the second subproblem ∇n_0 is applied but the particle remains stagnant. Let $\mathbf{F}_{ei}$, $\mathbf{F}_{di}$, and $\mathbf{F}_i$ be the electric force, the hydrodynamic force, and the total force acting on the particle in the z-direction in subproblem i, i = 1,2, respectively, and F_{ei}, F_{di}, and F_i be the corresponding magnitudes. As illustrated in Figure 1, $\mathbf{F_{e2}}$ comes from the effects of type I DLP, type II DLP, and electrophoresis, and $\mathbf{F_{d2}}$ comes from three types of osmotic flow. It can be shown that $F_1 = F_{e1} + F_{d1} = C_1U$[45] and $F_2 = F_{e2} + F_{d2} = C_2\nabla n_0$,[46] where C_1 and C_2 are proportional constants. Because $F_1 + F_2 = 0$ at steady state, we have

$$U = -\frac{F_2}{C_1} \tag{22}$$

If we let $F^*_{ei} = F_{ei}/\varepsilon\zeta^2$ and $F^*_{di} = F_{di}/\varepsilon\zeta^2$, then these scaled forces can be evaluated by[42,45,47]

$$F^*_{ei} = \iint_{S^*} \left[\frac{\partial \psi^*_e}{\partial n}\frac{\partial \delta\psi^*}{\partial Z} - \left(\frac{\partial \psi^*_e}{\partial t}\frac{\partial \delta\psi^*}{\partial t}\right) n_z \right] \mathrm{d}S^* \tag{23}$$

$$F^*_{di} = \iint_{S^*} (\sigma^*_{\mathbf{H}} \cdot \mathbf{n}) \cdot \mathbf{e}_z \, \mathrm{d}S^* \tag{24}$$

where $S^* = S/a^2$ is the scaled surface area with S being the surface area of the particle; n and t are the magnitude of the unit normal vector and that of the unit tangential vector, respectively; n_z is the z-component of n.

Numerical Procedure

The boundary-valued problem defined in eqs 1−21 is solved numerically by using a finite element method based software, *FlexPDE*.[34] The accuracy of the numerical results depend upon the mesh size. In particular, to obtain reliable results for the dependent variables in the membrane layer and in the double layer, the mesh density in those regions needs to be sufficiently high. In our case, if the number of element nodes exceeds ca. 4000, then the results are roughly mesh-independent with the percentage deviation smaller than 0.1%. Therefore, 6000 element nodes are used in the solution procedure, which involves the following steps. (i) An arbitrary particle velocity U_a is assumed, and the first subproblem solved, yielding F_{1a}, the total force acting on the particle in the first subproblem associated with the assumed particle velocity. (ii) Calculate the constant C_1 by $C_1 = F_{1a}/U_a$. (iii) The second subproblem is solved, yielding F_2, and the condition of $F_1 + F_2 = 0$ checked. If this is satisfied, then the solution procedure is completed. Otherwise, evaluate $U = F_2/C_1$ and then go back to step (i) with U_a replaced by U.

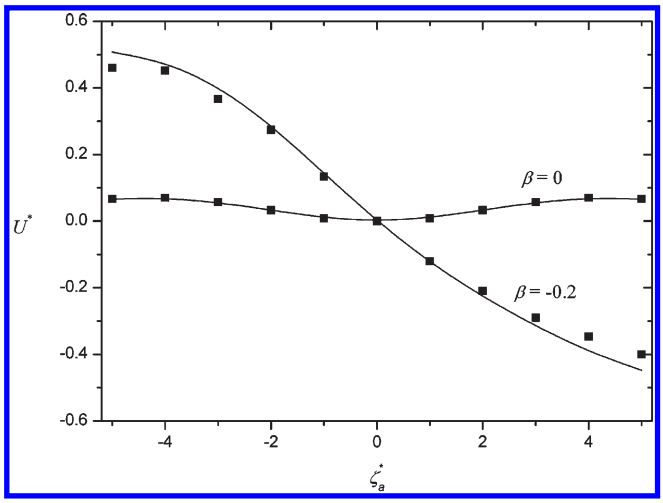

Figure 3. Variation of the scaled diffusiophoresis velocity of a soft particle U^* as a function of the scaled surface potential of its rigid core ζ^*_a. Solid curves: present numerical results at $\kappa a = 1$, $b/a = 8$, $c/a = 0.02$, $Q = 0$, and $\lambda a = 0.5$. Discrete symbols: numerical results for an isolated rigid sphere.[41]

To test the applicability of the present numerical procedure, it is used to solve the diffusiophoresis of an isolated rigid sphere in an infinite electrolyte solution previously solved numerically by Prieve and Roman.[41] To simulate the conditions of that problem, we let $b/a = 8$, $c/a = 0.02$, $Q = 0$, $\lambda a = 0.5$, and $\kappa a = 1$ in our case; that is, the disks are away from the particle and the membrane layer is thin and its friction coefficient small. Figure 3 shows the variation of the scaled diffusiophoresis velocity of the particle, $U^* = U/U_{ref}$, as a function of the scaled surface potential of its rigid core ζ^*_a. Both the present numerical results and the corresponding numerical results of Prieve and Roman[41] are presented. As seen in Figure 3, the present numerical procedure is capable of reproducing the result of Prieve and Roman.[41]

Results and Discussion

The diffusiophoretic behavior of the present soft particle under various conditions is examined by varying the thickness, the fixed charge density, the friction coefficient of its membrane layer, the thickness of double layer, and the diffusivities of ionic species. For illustration, we let $\gamma = 10^{-3}$, and, unless otherwise specified, we let $\zeta^*_a = 1$, $b/a = 5$, $c/a = 0.3$, $\lambda a = 5$, and $\kappa a = 1$.

Influence of Q and (c/a) on the Equilibrium Potential. Let us first examine the influence of the properties of the membrane layer of a particle on the equilibrium potential. Figure 4 shows the distribution of the scaled equilibrium potential ψ^*_e as a function of the scaled distance Z at $R = 0$. Because the surface of the rigid core of the particle is assumed to remain constant and the disks are uncharged, all the curves coincide at $Z = 1$ (upper pole of particle core) and $Z = 5$ (upper disk surface). Note that although the distribution of ψ^*_e for the case of $Q = 0$ in Figure 4a is the same as that for the case of $c/a = 0$ in Figure 4b, due to the presence of the membrane layer in the former, the velocity of the particle in the former is not the same as that in the latter. As seen in Figure 4a, where $c/a = 0.3$, the larger the $|Q|$, the larger the absolute value of the slope of ψ^*_e both inside and outside the membrane. Note that if $|Q|$ is sufficiently large, then ψ^*_e has a positive local maximum when $Q > 0$ and a negative local minimum when $Q < 0$. This phenomenon is important to the ionic distribution near the particle surface, where DLP occurs when

(44) O'Brien, R. W.; White, L. R. *J. Chem. Soc., Faraday Trans. II* **1978**, *74*, 1607.
(45) Happel, J.; Brenner, H. *Low Reynolds Number Hydrodynamics*; Martinus Nijhoff: Boston, 1983.
(46) Ebel, J. P.; Anderson, J. L.; Prieve, D. C. *Langmuir* **1988**, *4*, 396.
(47) Hsu, J. P.; Yeh, L. H. *J. Chin. Inst. Chem. Eng.* **2006**, *37*, 601.

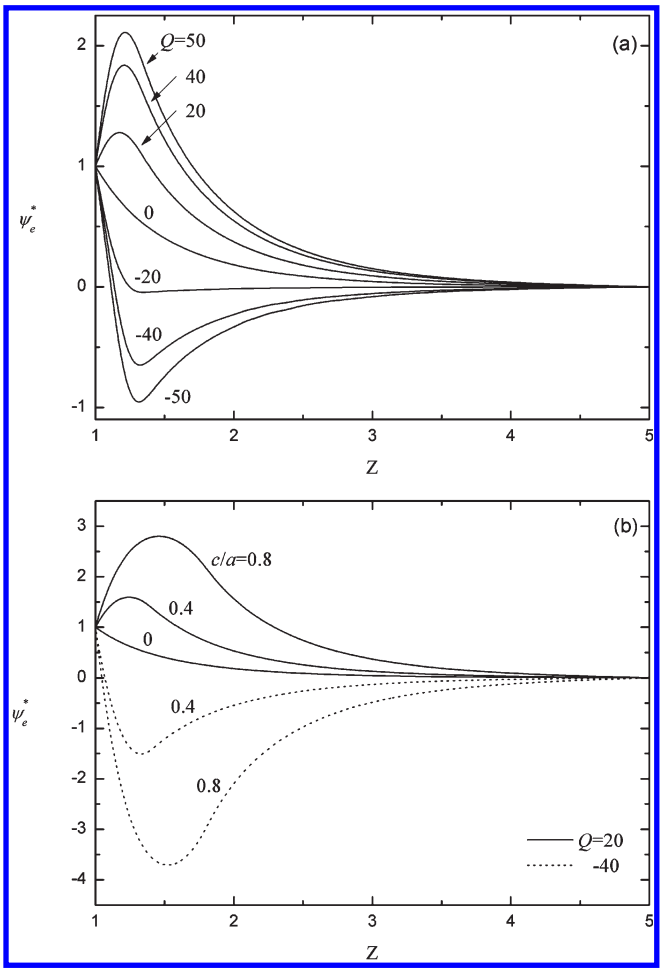

Figure 4. Spatial distribution of the scaled equilibrium potential ψ_e^* at $c/a = 0.3$ and $R = r/a = 0$ as a function of Z ($=z/a$) for various values of Q (a) and as a function of Z at various combinations of (c/a) and Q (b).

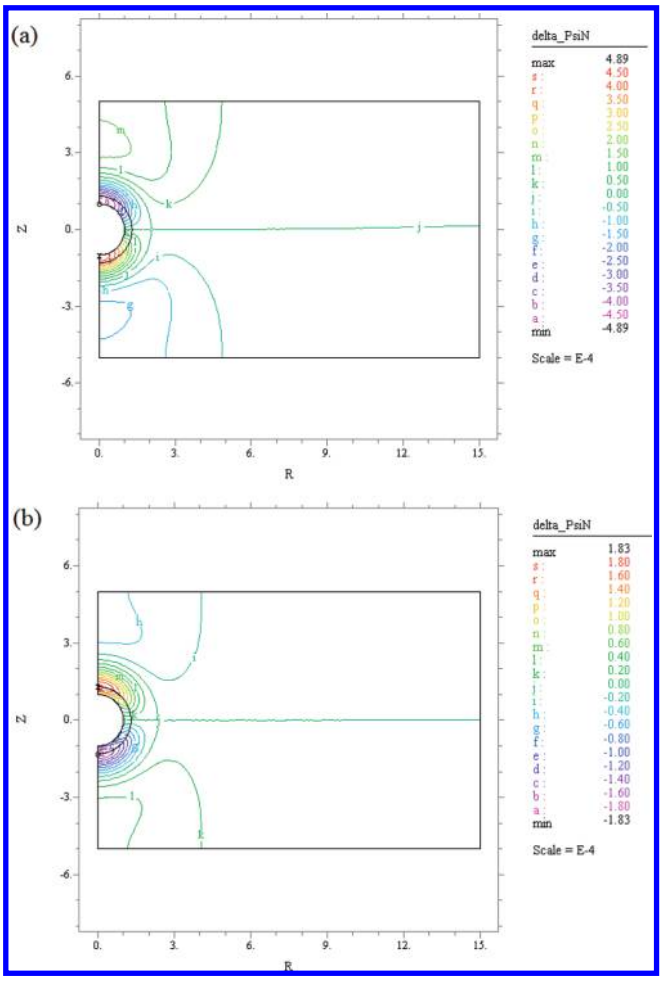

Figure 5. Contours of the scaled perturbed electric potential $\delta\psi^*$, denoted as delta_PsiN, for the case of Figure 4a on the half plane $\theta = \pi/2$ for two levels of Q at $\beta = 0$, $\kappa a = 1$, and (c/a) $= 0.3$. (a) $Q = 40$, (b) $Q = -40$.

∇n_0 is applied. Figure 4b illustrates the effects of the membrane thickness on the distribution of ψ_e^*. As seen, the maximum of $|\psi_e^*|$ occurs near the membrane−liquid interface, and the thicker the membrane layer the larger the $|\psi_e^*|$. We conclude that the electrical potential and, therefore, the diffusiophoretic behavior of a particle depend highly on the charged conditions and the thickness of its membrane layer.

It is known that the diffusivity of ionic species can play a role in diffusiophoresis.[16,36,41,46] To simulate its influence on the diffusiophoretic behavior of a particle, we consider two representative cases; namely, the liquid phase is an aqueous solution containing KCl and that containing NaCl. If $T = 298$ K, then because $\varepsilon = 8.854 \times 10^{-12} \times 80$ C/(Vm), $\eta = 0.993 \times 10^{-3}$ kg/(ms), $D_{K^+} \cong D_{Cl^-} \cong 2 \times 10^{-9}$ m^2/s, and $D_{Na^+} = 1.33 \times 10^{-9}$ m^2/s,[48] yielding $k_BT/z_1e = 0.02568$ V, $Pe_1 = Pe_2 = 0.235$, and $\beta \cong 0$ for the case of KCl, and $Pe_1 = 0.3525$, $Pe_2 = 0.235$, and $\beta = -0.2$ for the case of NaCl.

Case 1. Aqueous KCl Solution ($\beta \cong 0$). *Chemiphoresis.* In this case, the effect of electrophoresis is unimportant and the diffusiophoresis is driven mainly by chemiphoresis,[15] as is also proven by experimental observations.[46] Figure 5 illustrates the contours of the scaled perturbed electric potential $\delta\psi^*$ for the case of Figure 4a on the half plane $\theta = \pi/2$ at two levels of Q. Note that, due to the application of ∇n_0, the ionic concentration in the top region of the particle is higher than that in its bottom region. In the case of Figure 5a, the membrane layer of the particle is positively charged ($Q > 0$), so is its rigid core. The application of ∇n_0 makes the perturbed concentration of the anions (counterions) inside the double layer in the top region of the particle higher than that in its bottom region, yielding a negative (positive) $\delta\psi^*$ inside the double layer in the top (bottom) region of the particle. This is defined as type I DLP,[15] which induces a local electric field driving the particle toward the high-concentration side, that is, upward. Figure 5a also reveals that $\delta\psi^*$ is slightly positive immediately outside the double layer in the top region of the particle, implying that the perturbed concentration of cations (co-ions) there is slightly higher than that of anions (counterions), and the opposite trend is observed for $\delta\psi^*$ in the bottom region of the particle. This is defined as type II DLP,[15] which induces a local electric field driving the particle toward the low-concentration side, that is, downward. As pointed out by Hsu et al.,[15] the effect of type II DLP can be more important than that of type I DLP if ψ_e^* is sufficiently high (ca. 4) and κa is sufficiently large (ca. 5).

The membrane layer of the particle is negatively charged ($Q < 0$) in Figure 5b, and its rigid core is positively charged. In this case, although both types I and II DLP are still present, the distribution of $|\delta\psi^*|$ is not exactly the same as that in Figure 5a. For instance, the point at which the maximum of $|\delta\psi^*|$ occurs is near the core−membrane interface in Figure 5a but is near the membrane−liquid interface in Figure 5b. Note that, for a rigid

(48) Chun, B.; Ladd, A. J. C. *J. Colloid Interface Sci.* **2004**, *274*, 687.

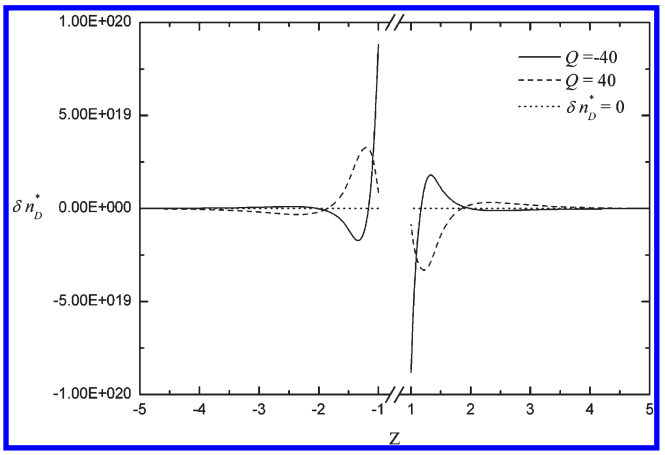

Figure 6. Spatial variation in the scaled net perturbed concentration difference δn_D^* ($= \delta n_1^* - \delta n_2^*$) as a function of Z at $R = 0$ for the case of Figure 5. (a) $Q = 40$, (b) $Q = -40$.

particle,[15] the degree of chemiphoresis, measured by $\delta\psi^*$, is independent of the sign of its surface charge, and for a soft particle comprising a charged membrane layer and an uncharged rigid core[13] $|\delta\psi^*|$ is also independent of the sign of the charge of its membrane layer.

To examine more deeply the influence of the charged conditions of the membrane layer of the particle on the spatial distribution of the ionic species, the variation of the scaled net perturbed concentration difference δn_D^* ($= \delta n_1^* - \delta n_2^*$) at $R = 0$ as a function of Z for the case of Figure 5 is plotted in Figure 6. Because $\kappa a = 1$ in this case, the double layer is in the interval of $1 < |Z| < 2$. On the right-hand side of Figure 6 (top-side of the particle or high-concentration side), $|\delta n_D^*|$ deviates from zero appreciably in the interval $2 < Z < 4$, which justifies the presence of type II DLP; the sign of δn_D^* depends upon that of Q. Figure 6 also shows the occurrence of type I DLP inside the double layer, where the behavior of δn_D^* near the core−membrane interface ($|Z| = 1$) depends highly on the sign of Q. For instance, at $Q = 40$, the membrane layer is positively charged, the perturbed concentration of anions is higher than that of cations, yielding a negative δn_D^* within that layer. If the membrane layer is negatively charged, the perturbed concentration of cations is usually much higher than that of anions inside that layer, yielding a positive δn_D^*. However, because the rigid core of the present particle is positively charged, anions tend to accumulate near the rigid core−membrane interface, yielding a negative δn_D^* and, therefore, a reduction in the degree of type I DLP. This is consistent with the result in Figure 5, where the $|\delta\psi^*|$ at $Q = -40$ is much lower than that at $Q = 40$. The distribution of δn_D^* on the left-hand side of Figure 6 (bottom-side of the particle or low-concentration side) is similar to that on its right-hand side except that the sign of δn_D^* becomes opposite.

Influence of λa, (c/a), and Q on the Diffusiophoretic Mobility. The dependence of the scaled diffusiophoresis velocity U^* on the scaled friction coefficient of the membrane layer, λa, and the scaled membrane thickness, (c/a), at various levels of Q is illustrated in Figure 7. The variation of λa arises, for example, from the variation in the total number of polymer segments in the membrane layer of a particle. This implies that, as λa varies, the corresponding hydrodynamic friction force for the fluid flow inside the membrane layer and, therefore, the velocity of the particle vary accordingly.[20] As seen in Figure 7a, the larger the λa, the smaller the U^*, which is expected because the larger the λa the greater the hydrodynamic friction force. Note that if λa is smaller

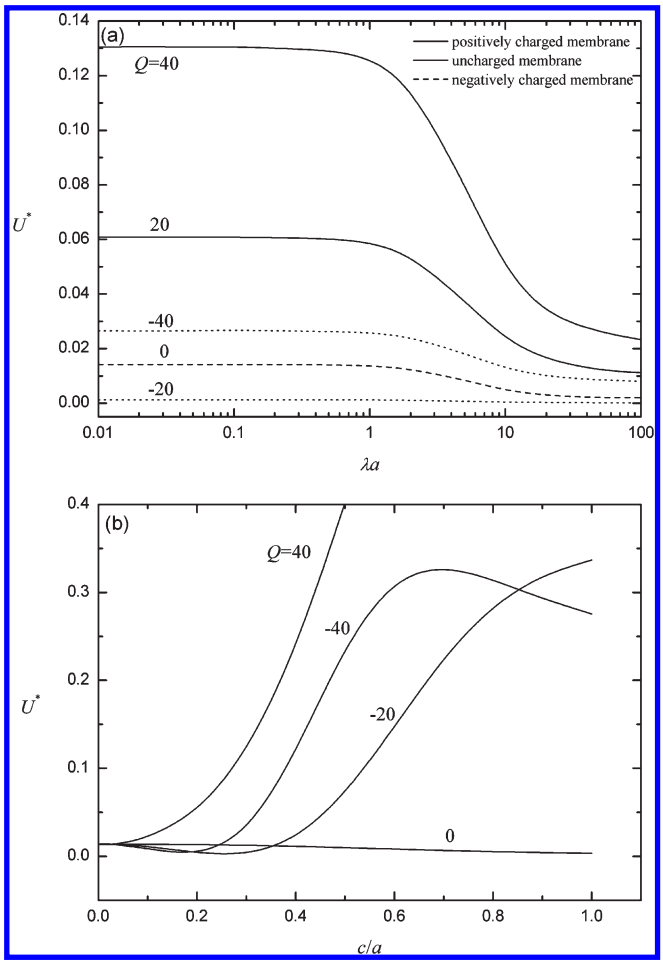

Figure 7. Variations of the scaled diffusiophoresis velocity U^* as a function of λa for various values of Q at $\beta = 0$ and $(c/a) = 0.3$ (a) and as a function of (c/a) at $\beta = 0$ and $\lambda a = 2$.

than ca. 0.5, the hydrodynamic friction force becomes unimportant, and U^* is essentially constant. On the other hand, if λa is larger than ca. 100, the membrane layer becomes almost impenetrable to fluid, and U^* is also roughly constant. As mentioned in the discussion of Figure 6, if the sign of the surface charge of the rigid core is different from that of the fixed charge in the membrane layer, the degree of type I DLP is reduced. This is also justified by Figure 7a, where $U^*(Q > 0)$ is larger than $U^*(Q < 0)$. Note that $U^*(Q = -20)$ is even smaller than $U^*(Q = 0)$, implying that the positive charge on the surface of the rigid core is screened essentially by the negative fixed charge in the membrane layer, as can be verified also by Figure 4a.

It is interesting to see in Figure 7b that the influence of the thickness of the membrane layer of a particle on its diffusiophoretic velocity depends highly upon the charged conditions of that layer. If the membrane layer is uncharged ($Q = 0$), the thicker that layer the greater the hydrodynamic friction force for the fluid flow inside, and therefore, U^* decreases monotonically with increasing (c/a). If the membrane layer is positively charged ($Q > 0$), because the thicker that layer the greater the amount of positive fixed charge, the more significant the type I DLP, and therefore, the larger the U^*. The variation of U^* with (c/a) becomes complicated if the membrane layer is negatively charged ($Q < 0$). For smaller values of (c/a), because the positive charge on the surface of the rigid core of the particle is screened by the negative fixed charge of its membrane layer, U^* decreases with increasing (c/a) and $U^*(Q < 0) < U^*(Q = 0)$. Since the amount

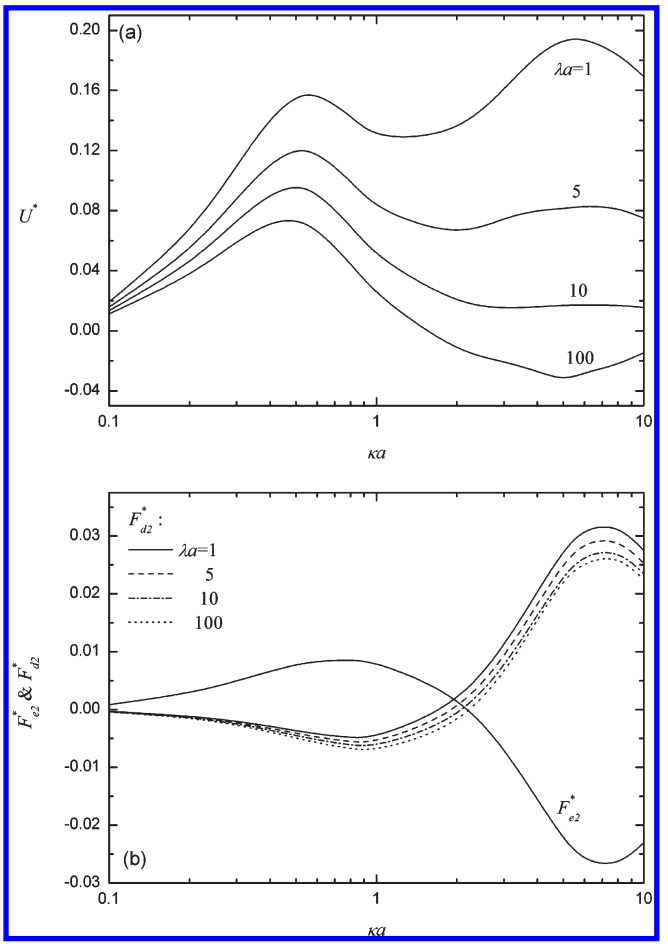

Figure 8. Variations of the scaled diffusiophoresis velocity U^* (a) and the scaled forces F^*_{e2} and F^*_{d2} (b) as a function of κa for various values of λa at $Q = 40$ and $\beta = 0$.

of negative fixed charge in the membrane layer increases with increasing (c/a), U^* becomes negative if (c/a) is sufficiently large. As (c/a) gets even larger, the electrophoretic behavior of the particle is dominated by the negative fixed charge of its membrane layer and the associated type I DLP tends to drive the particle toward the high-concentration side, and therefore, $|U^*|$ decreases with increasing (c/a), yielding a negative local minimum. A further increase in (c/a) makes U^* positive and increases with increasing (c/a). Figure 7b also suggests that if (c/a) is large, then U^* can have a positive local maximum as (c/a) varies, which results from the competition between type I and type II DLP.

Influence of λa and κa on the Diffusiophoretic Mobility. The variations of the scaled diffusiophoresis velocity U^* and the corresponding scaled forces in the second subproblem, F^*_{e2} and F^*_{d2}, as a function of κa at various values of λa are illustrated in Figure 8. Figure 8a reveals that the behavior of U^* as κa varies depends strongly on the value of λa: if λa is small, then U^* has two local maxima and a local minimum, and if λa is large, then U^* has only one local maximum and one local minimum. In addition, if λa is sufficiently large, the local minimum of U^* can be negative. These phenomena can be explained by the results presented in Figure 8b. This figure indicates that if κa is small, then type I DLP dominates, leading to a positive F^*_{e2}. As a result, the induced local electric field drives anions (counterions) toward the low-concentration side, yielding a negative F^*_{d2}; that is, a type I osmotic retardation flow is present, which is illustrated in Figure 9a. On the other hand, if κa is large, type II DLP becomes more important, yielding a negative F^*_{e2},

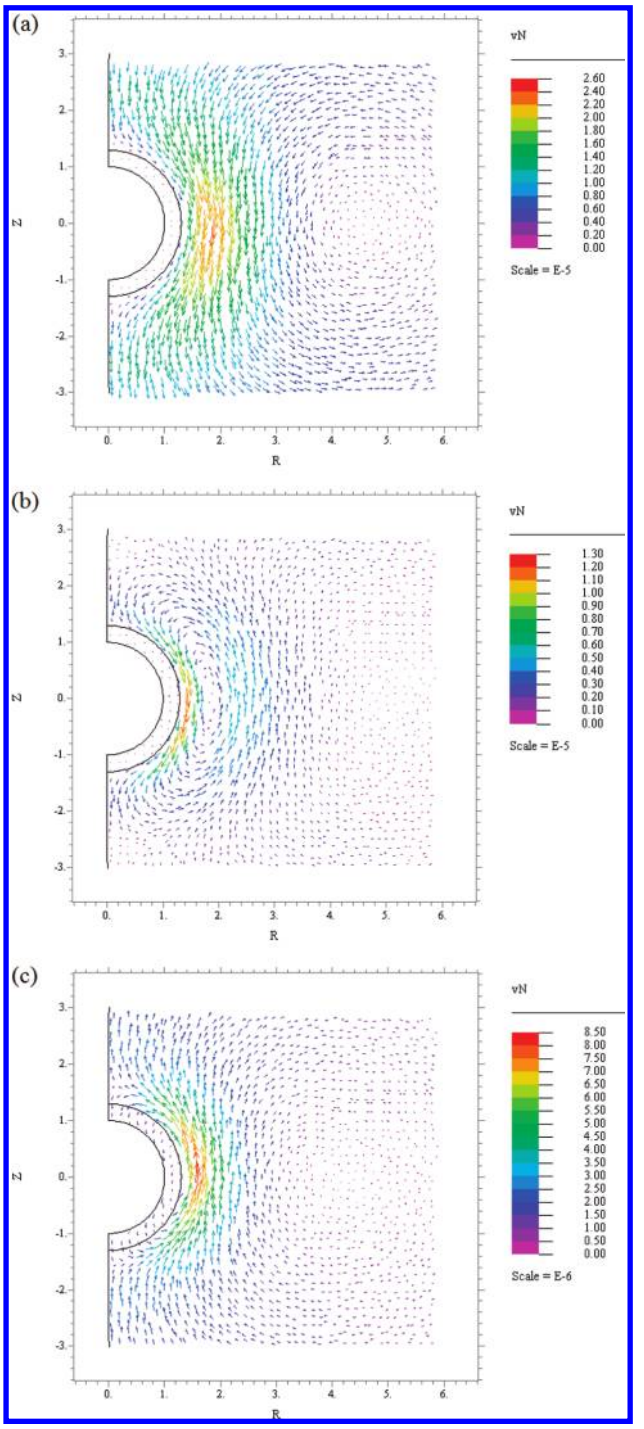

Figure 9. Scaled velocity field **v**, denoted as vN, on the half plane $\theta = \pi/2$ in the second subproblem for various values of κa for the case of Figure 8 at $\lambda a = 10$. (a) $\kappa a = 0.5$, (b) $\kappa a = 2$, and (c) $\kappa a = 8$.

and due to the presence of the associated type II osmotic retardation flow F^*_{d2} is positive, as seen in Figure 8b. This figure also reveals that if κa is fixed, then F^*_{e2} is essentially not influenced by λa, and therefore, the difference in U^* at different values of λa comes mainly from that in F^*_{d2}. Note that if $F^*_{d2} > 0$, then F^*_{d2} decreases with increasing λa, and if $F^*_{d2} < 0$, then $|F^*_{d2}|$ increases with increasing λa. This is because the mobile ions inside the membrane layer are mainly anions (counterions), and type I osmotic retardation flow always drives counterions toward the low-concentration side. Figure 9b,c suggests that if κa is sufficiently large,

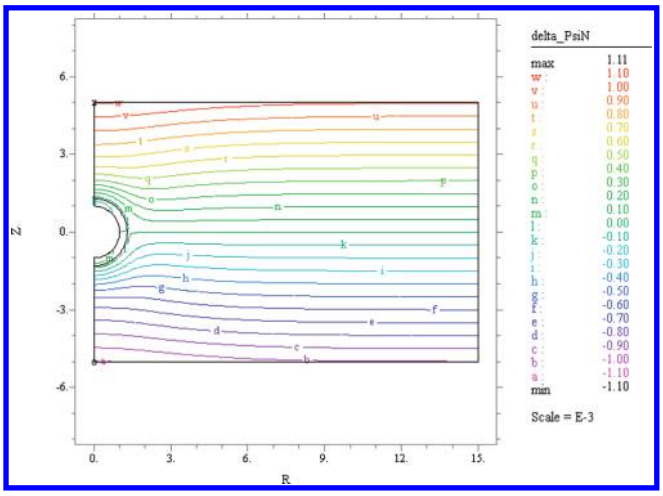

Figure 10. Contours of the scaled perturbed electric potential $\delta\psi^*$, denoted as delta_PsiN, on the half plane $\theta = \pi/2$ for the case where $\beta = -0.2$, $\kappa a = 1$, $(c/a) = 0.3$, and $Q = 20$.

although F^*_{d2} is dominated by type II osmotic retardation flow outside the membrane layer, the mobile ions inside that layer are still driven by type I osmotic retardation flow toward the low-concentration side. Note that as κa increases, both type II DLP and the associated type II osmotic retardation flow become more important.

Case 2. Aqueous NaCl Solution ($\beta = -0.2$). *Electrophoresis*. In this case, because $D_{Cl^-} > D_{Na^+}$, Cl^- diffuses faster than Na^+ and, therefore, the application of ∇n_0 induces a background electrical field driving a positively charged particle toward the low-concentration side, known as the electrophoresis effect.[14,15] The contours of the scaled perturbed electric potential $\delta\psi^*$ on the half plane $\theta = \pi/2$ for the case of $\beta = -0.2$ and $Q = 20$ are presented in Figure 10. As seen in this figure, the closer to the upper disk, the higher the level of $\delta\psi^*$; that is, the background electric field arising from electrophoresis effect directs to the lower disk. Note that the distribution of δn^*_D in the present case (not shown) is almost the same as that in Figure 6, where electrophoresis effect is absent. This implies that although electrophoresis effect is present, the chemiphoresis effects associated with types I and II DLP still yield a nonuniform distribution in $\delta\psi^*$ near the particle surface, as is seen in Figure 10. We conclude that, in the present case, the diffusiophoretic behavior of the particle is governed by the effects of chemiphoresis, the associated osmotic retardation flow, and electrophoresis. Note that the chemiphoresis is influenced strongly by the boundary.[14]

Influence of λa, (c/a), and Q on the Diffusiophoretic Mobility. The variations of the scaled diffusiophoresis velocity U^* at various combinations of λa, (c/a), and Q are illustrated in Figure 11. As stated previously, because $\beta \neq 0$ in the present case, the difference in the ionic diffusivities induces a background electric field, which drives a positively (negatively) charged particle toward the low- (high-) concentration side. Therefore, as seen in Figure 11a, if $Q > 0$, then $U^* < 0$, and the larger the Q the larger the $|U^*|$; if $Q < 0$ and $|Q|$ is sufficiently large, then $U^* > 0$ and the larger the $|Q|$ the larger the U^*. However, the electrophoresis effect is also accompanied by an electroosmotic retardation flow, which drives the counterions inside the membrane layer toward the direction opposite to that of the background electrical field. This effect can be justified by Figure 11a, where $|U^*|$ decreases with increasing λa. Note that if the membrane layer of the particle is uncharged ($Q = 0$), then it is driven toward the low-concentration side due to the positive surface potential of its

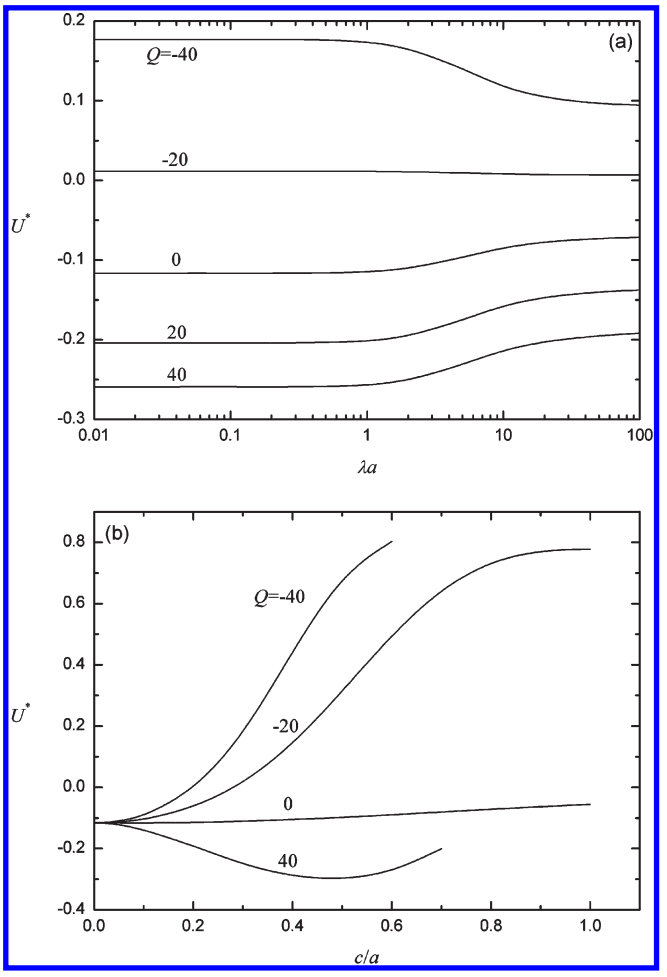

Figure 11. Variations of the scaled diffusiophoresis velocity U^* as a function of λa for various values of Q at $\beta = -0.2$ and $c/a = 0.3$ (a) and as a function of (c/a) at $\beta = -0.2$ and $\lambda a = 2$.

rigid core. Similar to the case of Figure 7a, if λa is either sufficiently large (ca. 100) or sufficiently small (ca. 1), then the velocity of the particle is roughly constant.

Figure 11b reveals that if $(c/a) \to 0$, that is, the membrane layer of the particle is infinitely thin, then because its rigid core is positively charged, it is driven by the background electric field toward the low-concentration side ($U^* < 0$). If the membrane layer of a particle is negatively charged ($Q < 0$), then both electrophoresis and chemiphoresis effects drive the particle toward the high-concentration side. In this case, the thicker the membrane layer the more the amount of fixed charge it carries, and therefore, the larger the $|U^*|$, as discussed in Figures 4b and 7b. Note that if the membrane layer is uncharged, because the larger the (c/a) the greater the friction for diffusiophoresis, $|U^*|$ becomes smaller. As seen in Figure 11b, if the membrane layer of the particle is positively charged ($Q = 40$), then $|U^*|$ increases with increasing (c/a), passes through a negative local minimum, and then decreases with a further increase in (c/a). The increase in $|U^*|$ in the first stage arises from that the thicker the membrane layer the more the amount of positively fixed charge it carries, and the decrease in $|U^*|$ in the last stage from that the electroosmotic retardation flow becomes important if the membrane layer is sufficiently thick. Note that if the membrane layer is positively charged ($Q > 0$), because the direction of the electric force coming from electrophoresis effect is opposite to that from chemiphoresis effect, the direction of diffusiophoresis depends upon which of these two effects dom-

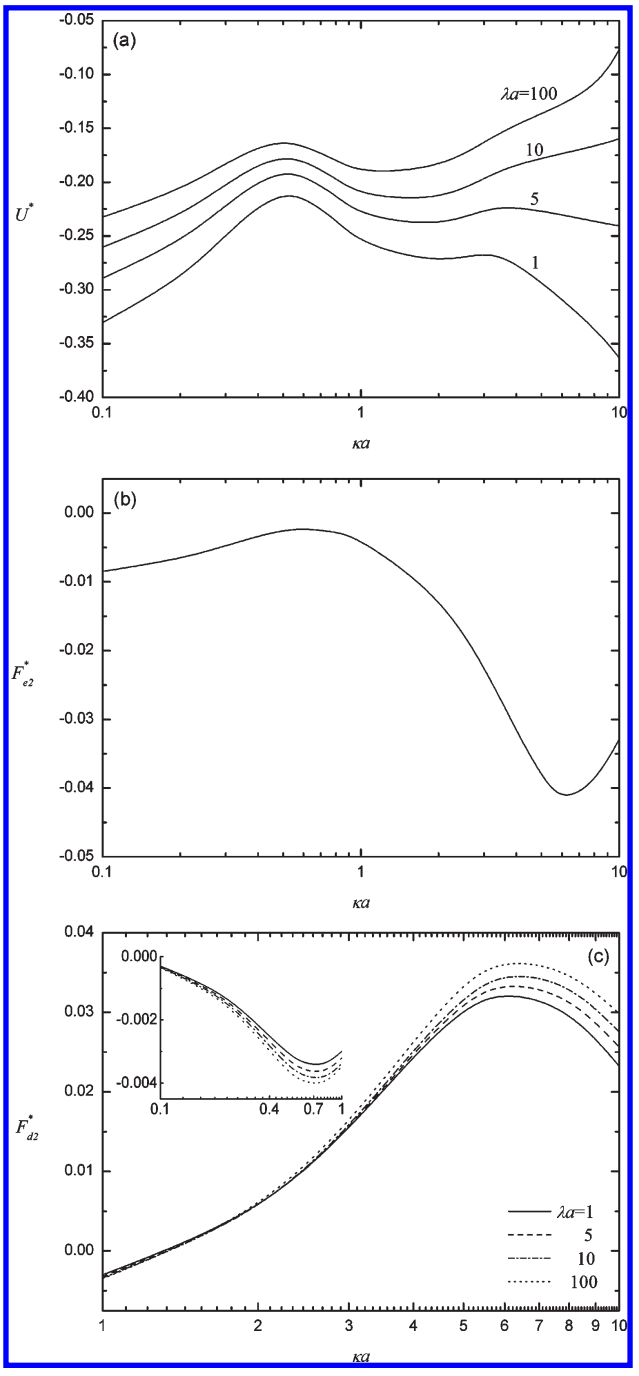

Figure 12. Variations of the scaled diffusiophoresis velocity U^* (a) and the scaled forces F^*_{e2} (b) and F^*_{d2} (c) as a function of κa for various values of λa at $Q = 40$ and $\beta = -0.2$.

inates. In general, if the boundary effect is insignificant and/or the double layer is thin, then the former is much more significant than the latter.[14]

Influence of λa and κa on the Diffusiophoretic Mobility. Figure 12 illustrates the variations of the scaled diffusiophoretic velocity U^* and the scaled forces F^*_{e2} and F^*_{d2} as a function of κa at various values of λa. As in the case of Figure 8, where $\beta = 0$, Figure 12 also suggests that the behavior of U^* as κa varies depends strongly upon the level of λa, that is, the magnitude of osmotic retardation force. As seen in Figure 12a, where the membrane layer of a particle is highly positively charged ($Q = 40$), the electrophoresis effect drives the particle toward the low-concentration side, and the larger the λa the smaller the $|U^*|$.

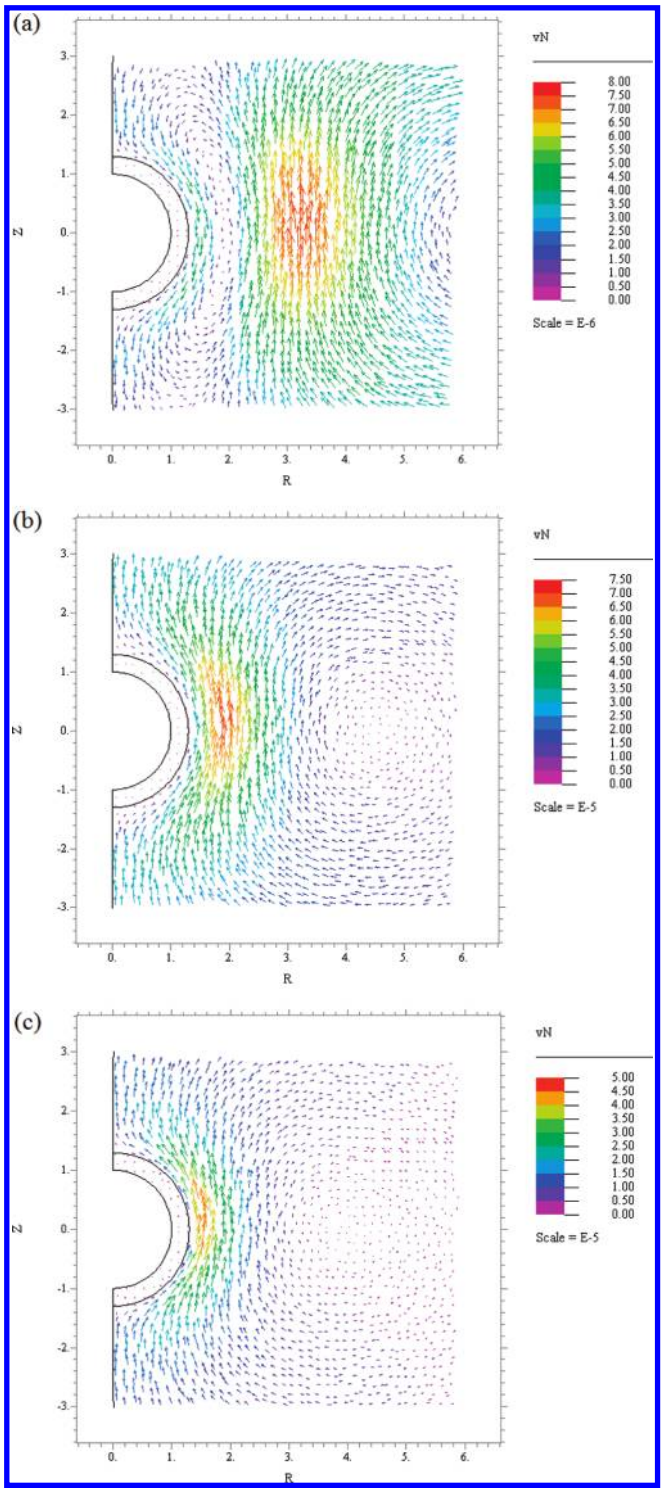

Figure 13. Scaled velocity field **v**, denoted as vN, on the half plane $\theta = \pi/2$ in the second subproblem for various values of κa for the case of Figure 13 at $\lambda a = 10$. (a) $\kappa a = 0.5$, (b) $\kappa a = 2$, and (c) $\kappa a = 8$.

A comparison between Figures 8b and 12b reveals that the presence of the electrophoresis effect in the latter makes the F^*_{e2} in the former shift down to become all negative in the latter, and the positive U^* in the former becomes negative in the latter. However, the shapes of the curves of F^*_{e2} in those two figures, which are insensitive to the variation in λa, are similar, implying that the chemiphoresis effect still plays a role. The behavior of U^* seen in Figure 12a results from the competition between F^*_{e2} and F^*_{d2}. In the present case, F^*_{d2} is contributed by both

chemiosmotic flow and electroosmotic retardation flow. The direction of the chemiosmotic flow associated with type I DLP is downward, that associated with type II is upward, and the direction of electroosmotic retardation flow is upward. Figure 12b and c reveals that if κa is small (thicker double layer), then both F_{e2}^* and F_{d2}^* are negative. Because type II DLP is insignificant in the present case, as discussed in Figure 8b, implying that the significance of type I osmotic retardation flow is comparable to that of electroosmosis. Since the membrane layer is positively charged, Figure 13a suggests that if the double layer is thick (small κa), then the osmotic retardation flow coming from type I DLP dominates. The presence of type I DLP is also justified by Figure 12b, where F_{e2}^* shows a negative local maximum at $\kappa a \cong 0.7$. Therefore, as seen in Figure 12c, if κa is small, then $|F_{d2}^*|$ increases with increasing λa, which is also seen in Figure 8b, where the electrophoresis effect is absent. Figure 13 reveals that as κa gets larger, the contribution of type I osmotic retardation flow becomes less significant. Note that the fluid velocity in Figure 13c is ca. 30 times that in Figure 13a, implying that the electroosmotic retardation flow is more important at larger κa. If κa exceeds ca. 1.5, then the hydrodynamic force is dominated by the electroosmotic flow resulting from the electrophoresis effect and type II osmotic retardation flow; type I osmotic retardation flow becomes relatively unimportant. As a result, F_{d2}^* becomes positive, and the larger the λa the greater the F_{d2}^*, which is opposite to the trend seen in Figure 8b. We conclude that, in an aqueous NaCl solution, the larger the λa the larger the $|F_{d2}^*|$, which is different from that in an aqueous KCl solution.

Figures 8 and 12 suggest that, through varying the thickness of double layer (by adjusting the bulk ionic concentration) and the friction coefficient of the membrane layer of a particle (by controlling the density of the polymer segment), it is possible for one to manipulate both the direction and the magnitude of the diffusiophoretic velocity of the particle. This is of much practical importance in the cases, for instance, where diffusiophoresis is adopted as a process for pattern formation or for the transport of drug.

Conclusions

We analyzed theoretically the diffusiophoresis of a soft particle comprising a rigid core and a porous membrane layer, which simulates biocolloids and rigid particles covered by an artificial membrane layer, in an electrolyte solution normal to two parallel disks. This simulates, for example, the deposition of a particle on a surface driven by a concentration gradient. We show that the chemiphoresis arising from the polarization of the double layer, the electrophoresis coming from the difference in the ionic diffusivities, and the associated osmotic flows can all play a role, yielding complicated diffusiophoretic behaviors. For instance, if the sign of the fixed charge of the membrane layer of a particle is opposite to the sign of the surface charge of its rigid core, then its diffusiophoretic velocity can be either smaller or larger compared to the corresponding rigid particle, depending upon the fixed charge density and/or the thickness of the membrane layer. In addition, both the sign and the magnitude of the diffusiophoretic velocity of a particle can be adjusted through varying the friction coefficient of its membrane layer. Furthermore, the flow pattern of the fluid in the vicinity of the particle can be controlled by selecting the types of ionic species and/or adjusting their concentrations. These results are of practical significance in the design of a diffusiophoresis operation or the interpretation of experimental data.

Acknowledgment. This work is supported by the National Science Council of the Republic of China.

List of Symbols

a	radius of the rigid core of a particle (m)
b	half the separation distance between two parallel disks (m)
C_1, C_2	proportional constants (-)
c	thickness of membrane layer (m)
D_j	diffusivity of ionic species j (m^2/s)
e	elementary charge (C)
$\mathbf{e_z}$	unit vector in the z-direction (-)
$\mathbf{F_{e2}}$, $\mathbf{F_{d2}}$, $\mathbf{F_2}$	the electric, hydrodynamic, and total force acting on a particle in sub-problem i (N)
F_{e2}, F_{d2}, F_2	the magnitudes of the forces $\mathbf{F_{e2}}$, $\mathbf{F_{d2}}$, $\mathbf{F_2}$ (N)
F_{e2}^*, F_{d2}^*, F_2^*	the scaled forces $F_{ei}/\varepsilon\zeta^2$, $F_{di}/\varepsilon\zeta^2$, $F_2/\varepsilon\zeta^2$ (-)
k_B	Boltzmann constant (J/K)
$\mathbf{n}$	unit normal vector (-)
n_{0e}	bulk concentration at equilibrium ($1/m^3$)
n_{j0e}	bulk concentration of ionic species j at equilibrium ($1/m^3$)
n_{je}, δn_j	equilibrium number concentration and perturbed number concentration of ionic species j ($1/m^3$)
$n_j = n_{je} + \delta n_j$	number concentration of ionic species j ($1/m^3$)
n_{je}^*, δn_j^*, n_j^*	scaled number concentrations n_{je}/n_{0e}, $\delta n_j/ n_{0e}$, n_j/n_{0e}(-)
$\delta n_D^* = \delta n_1^* - \delta n_2^*$	net perturbed number concentration difference (-)
∇_{n_0}	applied number concentration gradient ($1/m^4$)
p	pressure (Pa)
$Pe_j = \varepsilon\zeta^2/\eta D_j$	electric Peclet number of ionic species j (-)
$Q = \rho_{fix}a^2/\varepsilon\zeta$	scaled fixed charge density on the membrane layer (-)
r	radial coordinate (m)
R	$= r/a$ (-
T	absolute temperature (K)
U, $U_{ref} = \varepsilon\gamma\zeta^2/a\eta$	diffusiophoretic velocity and reference velocity (m/s)
$U^* = U/U_{ref}$	scaled diffusiophoretic velocity (-)
$\mathbf{v}$	relative velocity of the liquid phase (m/s)
$\mathbf{v}^*$ (vN)	$= \mathbf{v}/U_{ref}$ (-)
z	axial coordinate (m)
z_j	valences of ionic species j (-)
Z	$= z/a$ (-)
α	$= -z_2/z_1$ (-)
β	$= (D_1 - D_2)/(D_1 - \alpha D_2)$ (-)
ε	permittivity of water (C/V/m)
$\gamma = \nabla^* n_0^*$	scaled applied concentration gradient (-)
η	viscosity of liquid phase (kg/m/s)
$1/\kappa$	thickness of double layer, $=\{\Sigma_{j=1}^2[n_{j0e}(ez_j)^2/\varepsilon k_B T]\}^{-1/2}$ (m)

λ	reciprocal shielding length, $=(\tau/\eta)^{1/2}$ (1/m)
$\delta\mu_j$	perturbed electrochemical potential of ionic species j (J)
$\delta\mu_j^*$	$=\delta\mu_j/k_BT$ (-)
θ	angular coordinate (radian)
ρ_{fix}	fixed charge density of the membrane layer (C/m^3)
τ	friction coefficient inside the membrane layer (kg/m^3/s)
ψ_e	equilibrium electric potential (V)
$\delta\psi$ (delta_PsiN)	perturbed potential (V)
$\psi = \psi_e + \delta\psi$	electric potential (V)
ψ_e^*, $\delta\psi^*$, ψ^*	$=\psi_e/\zeta_a$, $\delta\psi/\zeta_a$, ψ/ζ_a (-)
$\zeta = k_BT/ez_1$	thermal potential (V)
ζ_a	surface potential of the rigid core (V)
ζ_a^*	$=\zeta_a/\zeta$ (-)